SIMULATION OPTIMIZATION SYSTEMS
Research Laboratory

SPACE MAPPING
OPTIMIZATION FOR
ENGINEERING DESIGN

J.W. Bandler, R.M. Biernacki, S.H. Chen,
R.H. Hemmers and K. Madsen

SOS–95–11–R

September 1995

**SPACE MAPPING
OPTIMIZATION FOR
ENGINEERING DESIGN**

J.W. Bandler, R.M. Biernacki, S.H. Chen,
R.H. Hemmers and K. Madsen

SOS-95-11-R

September 1995

SPACE MAPPING OPTIMIZATION FOR ENGINEERING DESIGN

J.W. BANDLER, R.M. BIERNACKI, S.H. CHEN, R.H. HEMMERS and K. MADSEN

Abstract. This contribution describes a novel theory called Space Mapping (SM) which is relevant to engineering optimization. Two approaches are presented: SM and aggressive SM. The SM technique utilizes a transformation between the input parameter spaces of different models of the same physical object. The aggressive SM technique employs a quasi-Newton iteration where approximations to the Jacobian matrix are updated by the classic Broyden formula. The SM technique has been successfully applied in the area of microwave circuit design. It is, however, applicable to a wide variety of problems where models of different complexity and computational intensity are available.

1. Introduction

This chapter describes a novel concept called Space Mapping (SM) [1-6]. The SM technique exploits a mathematical link between input parameters of different engineering models of the same physical object. Traditionally, there exists a number of engineering models of different types and levels of complexity to choose from. In the field of electronic circuits this may include equivalent circuit models, ideal and detailed empirical models, electromagnetic (EM) field theory based models, hybrid models [7], and even computational utilization of actual hardware measurements.

The SM concept is based on the alignment of two models: (1) a computationally efficient (fast) model which may lack the desired accuracy, and (2) an accurate but CPU-intensive model. This merger facilitates the demanding requirements of otherwise CPU-prohibitive design optimization within a practical time frame. This is accomplished by redirecting the optimization-related calculations to the first model while preserving the accuracy and confidence offered by a few well-targeted evaluations of the second model.

There are two phases in SM. In *Phase* 1, optimization is performed using the fast model to obtain its optimal performance. In *Phase* 2, a mapping between the input parameter spaces of the two models considered is iteratively established. Techniques such as least-squares or quasi-Newton steps are used to accomplish this. A distinct auxiliary optimization (parameter extraction) must be invoked in each iteration of *Phase* 2. This parameter extraction is used to determine the parameters of the fast model such that its response(s) match those of the reference response(s) obtained from

an evaluation of the accurate model. The uniqueness of the parameter extraction process is of utmost importance to the success of SM.

Our presentation describes the theoretical formulation of SM followed by a practical engineering example. First, we review the SM theory followed the aggressive SM strategy. As applied to electronic circuit design, we consider an equivalent empirical circuit model as the fast model. As the accurate model, we employ an extremely CPU-intensive model based on solving electromagnetic field equations. For illustration, we consider the design of a high-temperature superconducting (HTS) microstrip filter.

2. Space Mapping Optimization

Theory

Let the behaviour of a system be described by models in two spaces: the optimization space, denoted by X_{os}, and the EM (or validation) space, denoted by X_{em}. We represent the optimizable model parameters in these spaces by the vectors x_{os} and x_{em}, respectively. We assume that X_{os} and X_{em} have the same dimensionality, i.e., $x_{os} \in \mathbb{R}^n$ and $x_{em} \in \mathbb{R}^n$, but may not represent the same parameters. We assume that the X_{os}-space model responses, denoted by $R_{os}(x_{os})$, are much faster to calculate but less accurate than the X_{em}-space model responses, denoted by $R_{em}(x_{em})$.

The key idea behind SM optimization is the generation of an appropriate mapping, P, from the X_{em}-space to the X_{os}-space,

$$x_{os} = P(x_{em}),\qquad (2.1)$$

such that

$$R_{os}(P(x_{em})) \approx R_{em}(x_{em}).\qquad (2.2)$$

We assume that such a mapping exists and is one-to-one within some local modeling region encompassing our SM solution. We also assume that, based on (2.2), for a given x_{em} its image x_{os} in (2.1) can be found by a suitable parameter extraction procedure, and that this process is unique.

We initially perform optimization entirely in X_{os} to obtain the optimal solution x_{os}^*, for instance in the minimax sense [8], and subsequently use SM to find the mapped solution $\bar{x}_{em}$ in X_{em} as

$$\bar{x}_{em} = P^{-1}(x_{os}^*) \qquad (2.3)$$

once the mapping (2.1) is established. We designate $\bar{x}_{em}$ as the SM solution instead of x_{em}^* since the mapped solution represents only an approximation to the true optimum in X_{em}.

The mapping is established through an iterative process. We begin with a set of m X_{em}-space model base points

$$B_{em} = \{ x_{em}^{(1)}, x_{em}^{(2)}, ..., x_{em}^{(m)} \}. \qquad (2.4)$$

These initial m base points are selected in the vicinity of a reasonable candidate for the X_{em}-space model solution. For example, if x_{em} and x_{os} consist of the same physical parameters, then the set B_{em} can be chosen as

$$x_{em}^{(1)} = x_{os}^*, \qquad (2.5)$$

with the remaining $m-1$ base points chosen arbitrarily by perturbation as

$$x_{em}^{(i)} = x_{em}^{(1)} + \Delta x_{em}^{(i-1)}, \quad i = 2, 3, ..., m. \qquad (2.6)$$

Once the set B_{em} is chosen, we perform EM analyses at each base point to obtain the X_{em}-space model responses $R_{em}(x_{em}^{(i)})$ for $i = 1, 2, ..., m$. This is followed by parameter extraction optimization in X_{os} to obtain the corresponding set of m X_{os}-space model base points

$$B_{os} = \{ x_{os}^{(1)}, x_{os}^{(2)}, ..., x_{os}^{(m)} \}. \qquad (2.7)$$

The parameter extraction process is carried out by the following optimization:

$$\underset{x_{os}^{(i)}}{\text{minimize}} \, \| R_{os}(x_{os}^{(i)}) - R_{em}(x_{em}^{(i)}) \| \qquad (2.8)$$

for $i = 1, 2, ..., m$ where $\| \cdot \|$ indicates a suitable norm. The additional $m-1$ points apart from $x_{em}^{(1)}$ are required merely to establish full-rank conditions leading to the initial approximation of the mapping (denoted by P_0 - its exact construction is explained later).

At the jth iteration, both sets may be expanded to contain, in general, m_j points which are used to establish the updated mapping P_j. Since the analytical form of P is not available, we use the current approximation P_j to estimate $\bar{x}_{em}$ in (2.3), i.e.,

3

$$x_{em}^{(m_j+1)} = P_j^{-1}(x_{os}^*).$$ (2.9)

The process continues iteratively until the termination condition

$$\| R_{os}(x_{os}^*) - R_{em}(x_{em}^{(m_j+1)}) \| \leq \epsilon$$ (2.10)

is satisfied, where ϵ is a small positive constant. If so, P_j is our desired P. If not, the set of base points in B_{em} is augmented by $x_{em}^{(m_j+1)}$ and correspondingly, $x_{os}^{(m_j+1)}$ determined by (2.8) augments the set of base points in B_{os}. Upon termination, we set $\overline{x}_{em} = x_{em}^{(m_j+1)} = P_j^{-1}(x_{os}^*)$ as the SM solution. This process is illustrated graphically in Fig. 1

We define each of the transformations P_j as a linear combination of some predefined and fixed fundamental functions

$$\hat{f}_1(x_{em}), \hat{f}_2(x_{em}), \hat{f}_3(x_{em}), \ldots, \hat{f}_t(x_{em})$$ (2.11)

such that

$$x_{os_i} = \sum_{s=1}^{t} a_{is} \hat{f}_s(x_{em})$$ (2.12)

or, in matrix form

$$x_{os} = P_j(x_{em}) = A_j \hat{f}(x_{em})$$ (2.13)

where A_j is a $n \times t$ matrix, $\hat{f}(x_{em})$ is a t-dimensional column vector of fundamental functions and $m_j \geq t$.

Consider the mapping P_j for all points in the sets B_{em} and B_{os}. Expanding (2.13) gives

$$\left[x_{os}^{(1)} \ x_{os}^{(2)} \ \ldots \ x_{os}^{(m_j)} \right] \quad A_j \left[\hat{f}(x_{em}^{(1)}) \ \hat{f}(x_{em}^{(2)}) \ \ldots \ \hat{f}(x_{em}^{(m_j)}) \right].$$ (2.14)

For a linear mapping, $\hat{f}(x_{em})$ contains the $n+1$ linear functions: $1, x_1, x_2, \ldots, x_n$. Hence, (2.14) can be written as

$$\left[x_{os}^{(1)} \ x_{os}^{(2)} \ \ldots \ x_{os}^{(m_j)} \right] = Q_j \left[x_{em}^{(1)} \ x_{em}^{(2)} \ \ldots \ x_{em}^{(m_j)} \right] + \left[b_j \ b_j \ \ldots \ b_j \right]$$

$$= \left[b_j \ Q_j \right] \begin{bmatrix} 1 & 1 & \ldots & 1 \\ x_{em}^{(1)} & x_{em}^{(2)} & \ldots & x_{em}^{(m_j)} \end{bmatrix}$$ (2.15)

where Q_j is an $n \times n$ matrix and b_j is an $n \times 1$ column vector. Let us define

4

$$C = \left[x_{os}^{(1)} \ x_{os}^{(2)} \ ... \ x_{os}^{(m_j)} \right]^T, \tag{2.16}$$

$$D = \left[\hat{f}(x_{em}^{(1)}) \ \hat{f}(x_{em}^{(2)}) \ ... \ \hat{f}(x_{em}^{(m_j)}) \right]^T = \begin{bmatrix} 1 & 1 & ... & 1 \\ x_{em}^{(1)} & x_{em}^{(2)} & ... & x_{em}^{(m_j)} \end{bmatrix}^T \tag{2.17}$$

and

$$A_j = \left[b_j \ Q_j \right]. \tag{2.18}$$

Then (2.14) can be rewritten as

$$C^T = A_j D^T \tag{2.19}$$

and transposing both sides gives

$$D A_j^T = C. \tag{2.20}$$

Augmenting (2.20) by some weighting factors defined by an $m_j \times m_j$ diagonal matrix W, where

$$W = diag\{w_i\} \tag{2.21}$$

gives

$$W D A_j^T = W C. \tag{2.22}$$

The least-squares solution to this system is

$$A_j^T = \left(D^T W^T W D \right)^{-1} D^T W^T W C. \tag{2.23}$$

Larger/smaller weighting factors emphasize/deemphasize the influence of the corresponding base points on the SM transformation.

Implementation

We now present a straightforward implementation of the SM algorithm. First, begin with a point, $x_{os}^* \triangleq arg\,min\{H(x_{os})\}$, representing the optimal solution in X_{os} where $H(x_{os})$ is some appropriate objective function. Then, the algorithm proceeds as follows:

Step 0. Initialize $x_{em}^{(1)} = x_{os}^*$. If $\| R_{os}(x_{os}^*) - R_{em}(x_{em}^{(1)}) \| \leq \epsilon$, stop. Otherwise, initialize $\Delta x_{em}^{(i-1)}$ for $i = 2, 3, ..., m$.

5

Step 1. Select $m-1$ additional base points in X_{em} by perturbation, i.e., $x_{em}^{(i)} = x_{em}^{(1)} + \Delta x_{em}^{(i-1)}$ for $i = 2, 3, ..., m$.

Step 2. Perform parameter extraction optimization to obtain $x_{os}^{(i)}$ for $i = 1, 2, ..., m$.

Step 3. Initialize $j = 0$, $m_j = m$.

Step 4. Compute $A_j^T = \left(D^T W^T W D\right)^{-1} D^T W^T W C$ and extract the matrix Q_j and the vector b_j according to $A_j = \begin{bmatrix} b_j & Q_j \end{bmatrix}$.

Step 5. Set $x_{em}^{(m_j+1)} = Q_j^{-1}(x_{os}^* - b_j)$.

Step 6. If $\| R_{os}(x_{os}^*) - R_{em}(x_{em}^{(m_j+1)}) \| \leq \epsilon$, stop.

Step 7. Perform parameter extraction optimization to obtain $x_{os}^{(m_j+1)}$.

Step 8. Augment the matrix C with $x_{os}^{(m_j+1)}$ and the matrix D with $x_{em}^{(m_j+1)}$.

Step 9. Set $j = j + 1$, $m_j = m_j + 1$; go to *Step* 4.

Comments

Note, that in *Steps* 2 and 7 an auxiliary optimization (parameter extraction) is invoked. In *Step* 5, $x_{em}^{(m_j+1)}$ may be snapped to the closest grid point if the EM simulator uses a fixed-grid meshing scheme.

3. Aggressive Space Mapping Optimization

Theory

Consider an important property of the termination condition in (2.10). When approaching the SM solution, the X_{em}-space model response $R_{em}(x_{em}^{(m_j+1)})$ will closely match the optimal X_{os}-space model response $R_{os}(x_{os}^*)$, within some tolerance ϵ. Hence, after performing an additional parameter extraction optimization in X_{os}, the resulting point $x_{os}^{(m_j+1)} = P(x_{em}^{(m_j+1)})$ approaches the point x_{os}^*. Stated more precisely, as $j \to M$, $x_{os}^{(m_j+1)} \to x_{os}^*$, or

$$\| x_{os}^{(m_j+1)} - x_{os}^* \| \leq \eta \quad \text{as} \quad j \to M \tag{3.1}$$

where η is a small positive constant and M is the number of iterations needed to converge to an SM solution.

Based on this observation, we can now formulate the aggressive SM approach. From (2.1), we assume that the vector of X_{os}-space model parameters is a nonlinear vector function, P, of the X_{em}-space model parameters. We define our goal by setting η to 0 in (3.1). Hence, we consider the set of n nonlinear equations

$$f(x_{em}) = 0 \tag{3.2}$$

where

$$f(x_{em}) = P(x_{em}) - x_{os}^* \tag{3.3}$$

and x_{os}^* is a given vector (optimal solution in X_{os}).

Let $x_{em}^{(j)}$ be the jth approximation to the solution of (3.2) and $f^{(j)}$ written for $f(x_{em}^{(j)})$. The next iterate $x_{em}^{(j+1)}$ is found by a quasi-Newton iteration

$$x_{em}^{(j+1)} = x_{em}^{(j)} + h^{(j)} \tag{3.4}$$

where $h^{(j)}$ solves the linear system

$$B^{(j)} h^{(j)} = -f^{(j)}. \tag{3.5}$$

$B^{(j)}$ is an approximation to the Jacobian matrix

$$J(x_{em}^{(j)}) = \left[\frac{\partial f^T(x_{em})}{\partial x_{em}} \right]^T \Bigg|_{x_{em} = x_{em}^{(j)}} \tag{3.6}$$

and is established based on the results from all previous iterations. In our implementation, $B^{(1)}$ is set to the identity matrix. The approximation to the Jacobian matrix is updated by the classic Broyden formula [9]

$$B^{(j+1)} = B^{(j)} + \frac{f(x_{em}^{(j)} + h^{(j)}) - f(x_{em}^{(j)}) - B^{(j)} h^{(j)}}{h^{(j)^T} h^{(j)}} h^{(j)^T}. \tag{3.7}$$

Incorporating (3.5) into (3.7) gives a simplified updating formula

$$B^{(j+1)} = B^{(j)} + \frac{f^{(j+1)} h^{(j)^T}}{h^{(j)^T} h^{(j)}} \tag{3.8}$$

where $f^{(j+1)}$ is obtained by evaluating (3.3) at $x_{em}^{(j+1)}$ using the parameter extraction optimization described in (2.8). This process is illustrated graphically in Fig. 2.

This approach is significantly more efficient than the original SM algorithm. We avert from performing time-consuming and possibly unproductive EM analyses at the perturbed points around the starting point. Instead, we begin with a straightforward initial estimate and attempt to improve the EM solution in a systematic manner.

Implementation

As before, begin with a point, $x_{os}^* \triangleq arg\ min\{H(x_{os})\}$, representing the optimal solution in X_{os} where $H(x_{os})$ is some appropriate objective function. Then, the algorithm proceeds as follows:

Step 0.   Initialize $x_{em}^{(1)} = x_{os}^*$, $B^{(1)} = 1$, $f^{(1)} = P(x_{em}^{(1)}) - x_{os}^*$, $j = 1$. Stop if $\| f^{(1)} \| \le \eta$.

Step 1.   Solve $B^{(j)} h^{(j)} = -f^{(j)}$ for $h^{(j)}$.

Step 2.   Set $x_{em}^{(j+1)} = x_{em}^{(j)} + h^{(j)}$.

Step 3.   Perform parameter extraction optimization to get $x_{os}^{(j+1)}$, i.e., evaluate $P(x_{em}^{(j+1)})$.

Step 4.   Compute $f^{(j+1)} = P(x_{em}^{(j+1)}) - x_{os}^*$. If $\| f^{(j+1)} \| \le \eta$, stop.

Step 5.   Update $B^{(j)}$ to $B^{(j+1)}$.

Step 6.   Set $j = j + 1$; go to *Step* 1.

Comments

In *Steps* 0 and 3, an auxiliary optimization (parameter extraction) is invoked to evaluate $P(x_{em}^{(j+1)})$. In *Step* 2, $x_{em}^{(j+1)}$ may be snapped to the closest grid point if the EM simulator uses a fixed-grid meshing scheme. If this is the case, *Step* 5 should employ (3.7) as the updating formula.

In our previous work [5, 6], the Space Mapping concept has been applied to the parameter extraction process, overcoming severely misaligned responses induced by inadequate empirical models. Although not discussed here, that approach was used at the starting point for the optimization problem discussed in Section 4.

4. Design of a High-temperature Superconducting (HTS) Parallel Coupled-line Microstrip Filter Exploiting Aggressive Space Mapping

The SM technique has been successfully applied to the design of an HTS filter. A detailed description of the filter (see Fig. 3) can be found in [2, 4-6]. This relatively small circuit exemplifies difficulties in directly using detailed EM simulations during optimization. To obtain an accurate and detailed circuit response, such as the one shown in Fig. 5, one needs more than a week of CPU time on a SPARCstation 10. To invoke such simulations many times during optimization is prohibitive.

For this problem, we consider 6 optimization variables representing the geometrical dimensions of the filter. We employ two models: (1) a fast model, based on empirical formulas available in the OSA90/hope [10] software package, and (2) an accurate but extremely CPU-intensive model, based on solving electromagnetic field equations by the *em* simulator [11].

Following *Phase* 1 of SM, we optimize the HTS filter using the OSA90/hope empirical model. The optimization goal is formulated in terms of the so-called scattering parameters S. These S parameters quantify the filter behaviour in terms of the power transfer from the input to the output of the filter [12]. Of particular interest is the parameter $|S_{21}|$ and its dependence on frequency (frequency response). The filtering capabilities of the circuit considered are described by the design specifications:

$$|S_{21}| \leq 0.05 \qquad \text{in the stopband}$$
$$|S_{21}| \geq 0.95 \qquad \text{in the passband}$$

where the stopband includes frequencies below 3.967 GHz and above 4.099 GHz and the passband lies in the frequency range [4.008 GHz, 4.058 GHz]. An appropriate objective function for optimization is formulated from the design specifications [8].

Fig. 4 shows the $|S_{21}|$ (and $|S_{11}|$) empirical model responses after performing minimax optimization using OSA90/hope. The *em* simulated frequency response differs significantly from that of the empirical model, as shown in Fig. 5.

In *Phase* 2 of SM, our aim is to establish a mapping in order to find a solution in the EM space which substantially reproduces the performance predicted by the optimal empirical model.

9

In this phase, in order to further reduce the CPU time of EM simulations, we do not consider as fine frequency sweeps as those shown in the figures. We use only 15 frequency points per sweep which turned out to be adequate. The SM solution emerges after only six such simplified EM analyses. Fig. 6 compares the filter responses of the optimal empirical model and the *em* simulated SM solution. Fig. 7 shows the progress of the aggressive SM algorithm as applied to the HTS filter design.

5. Conclusions

This presentation has included a theoretical formulation of the Space Mapping technique and an improved aggressive Space Mapping approach. The aggressive Space Mapping theory has been illustrated by the design optimization of a high-temperature superconducting parallel coupled-line microstrip filter.

Space Mapping optimization is a newly emerging and very promising approach. It exploits the speed of an efficient model and blends it with a few slow but highly accurate model evaluations to effectively perform design optimization within a practical time frame. A few recent publications in the engineering field exhibit some similarities to concepts found in Space Mapping [13-16].

In the near future we expect to see the Space Mapping concept applied to active devices. In this domain, physics-based models and physical models will be utilized [17]. Physics-based models relate the equivalent circuit elements to the device physics based on simplified analytical solutions of device equations. Physical models, based on the numerical solution of fundamental device equations are the most accurate. However, they require significantly more computation time than the physics-based models. Hence, Space Mapping may be the key to achieving the accuracy of physical simulation and the speed of circuit-level optimization.

Surprisingly, the concept of Space Mapping is only now establishing itself in the domain of circuit optimization. This is despite the overwhelming array of engineering models of devices, circuits and systems. It should be noted that designers increasingly employ accurate CPU-intensive

simulators, yet extensive use of efficient simplified models is made to avoid time-consuming analyses. SM bridges the two approaches and takes advantage of their respective benefits.

It is of interest to study concepts such as robustness, convergence and flexibility (using models with different physical parameters) in relation to Space Mapping optimization.

6. References

[1]   J.W. Bandler, R.M. Biernacki, S.H. Chen, P.A. Grobelny and R.H. Hemmers, "Space mapping technique for electromagnetic optimization," *IEEE Trans. Microwave Theory Tech.*, vol. 42, 1994, pp. 2536-2544.

[2]   J.W. Bandler, R.M. Biernacki, S.H. Chen, W.J. Getsinger, P.A. Grobelny, C. Moskowitz and S.H. Talisa, "Electromagnetic design of high-temperature superconducting microwave filters," *Int. J. Microwave and Millimeter-Wave Computer-Aided Engineering*, vol. 5, 1995, pp. 331-343.

[3]   J.W. Bandler, R.M. Biernacki, S.H. Chen, P.A. Grobelny and R.H. Hemmers, "Exploitation of coarse grid for electromagnetic optimization," *IEEE MTT-S Int. Microwave Symp. Dig.* (San Diego, CA), 1994, pp. 381-384.

[4]   J.W. Bandler, R.M. Biernacki, S.H. Chen, P.A. Grobelny, C. Moskowitz and S.H. Talisa, "Electromagnetic design of high-temperature superconducting microwave filters," *IEEE MTT-S Int. Microwave Symp. Dig.* (San Diego, CA), 1994, pp. 993-996.

[5]   J.W. Bandler, R.M. Biernacki, S.H. Chen, R.H. Hemmers and K. Madsen, "Electromagnetic optimization exploiting aggressive space mapping," *IEEE Trans. Microwave Theory Tech.*, vol. 43, 1995, pp. xxx-xxx.

[6]   J.W. Bandler, R.M. Biernacki, S.H. Chen, R.H. Hemmers and K. Madsen, "Aggressive space mapping for electromagnetic design," *IEEE MTT-S Int. Microwave Symp. Dig.* (Orlando, FL), 1995, pp. 1455-1458.

[7]   D.G. Swanson, Jr., "Using a microstrip bandpass filter to compare different circuit analysis techniques," *Int. J. Microwave and Millimeter-Wave Computer-Aided Engineering*, vol. 5, 1995, pp. 4-12.

[8]   J.W. Bandler and S.H. Chen, "Circuit optimization: the state of the art," *IEEE Trans. Microwave Theory Tech.*, vol. 36, 1988, pp. 424-443.

[9]   C.G. Broyden, "A class of methods for solving nonlinear simultaneous equations," *Math. of Comp.*, vol. 19, 1965, pp. 577-593.

[10]   *OSA90/hope*™ and *Empipe*™, Optimization Systems Associates Inc., P.O. Box 8083, Dundas, Ontario, Canada L9H 5E7, 1994.

[11]   *em*™ and *xgeom*™, Sonnet Software, Inc., 135 Old Cove Road, Suite 203, Liverpool, NY 13090-3774, 1994.

[12]   D.M. Pozar, *Microwave Engineering*, Addison-Wesley, 1990.

11

[13]   V.V. Toropov, "Simulation approach to structural optimization," Structural Optimization, vol. 1, 1989, pp. 37-46.

[14]   V.V. Toropov, A.A. Filatov and A.A. Polynkin, "Multiparameter structural optimization using FEM and multipoint explicit approximations," Structural Optimization, vol. 6, 1993, pp. 7-14.

[15]   A.A. Giunta, V. Balabanov, M. Kaufman, S. Burgee, B. Grossman, R.T. Haftka, W.H Mason and L.T. Watson, "Variable-complexity response surface design of an HSCT configuration," *Proceedings of the ICASE/LaRC Workshop on Multidisciplinary Design Optimization.* (Hampton, VA), 1995.

[16]   S. Burgee, A.A. Guinta, R. Narducci, L.T. Watson, B. Grossman and R.T. Haftka, "A coarse grained variable-complexity approach to MDO for HSCT design," in *Parallel Processing for Scientific Computing*, D.H. Bailey, P.E. Bjørstad, J.R. Gilbert, M.V. Mascagni, R.S. Schreiber, H.D. Simon, V.J. Torczon and L.T. Watson (eds.), SIAM, Philadelphia, PA, 1995, pp. 96-101.

[17]   J.W. Bandler, "Statistical modeling, design centering, yield optimization and cost-driven design," *CAD Design Methodology for Commercial Applications.* Workshop WFFE (A.M. Pavio, Organizer and Chairman), IEEE MTT-S Int. Microwave Symp. (Orlando, FL), 1995.
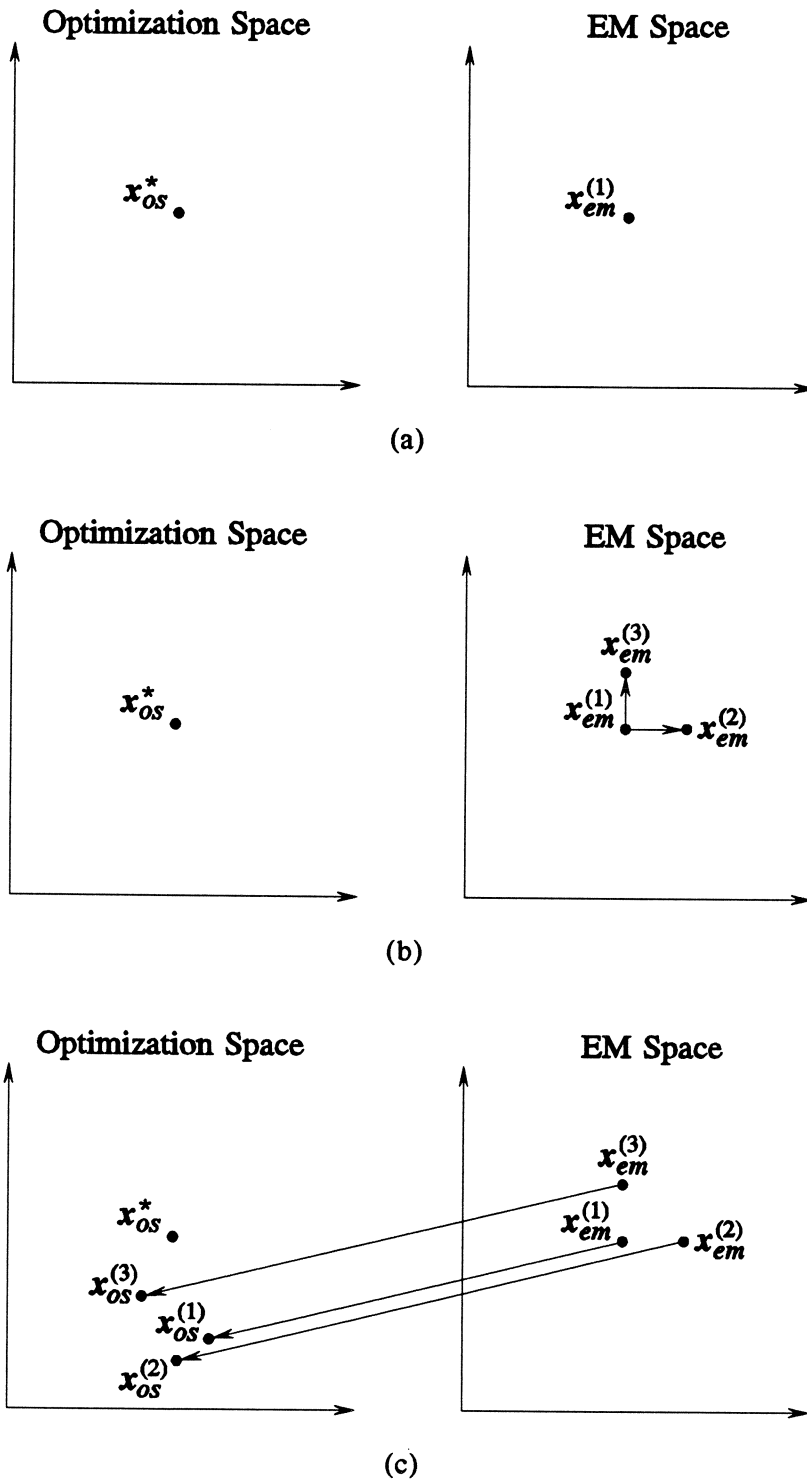
Fig. 1. Illustration of Space Mapping optimization: (a) set $x_{em}^{(1)} = x_{os}^*$, assuming x_{em} and x_{os} represent the same physical parameters, (b) generate additional base points around $x_{em}^{(1)}$, (c) perform X_{os}-space model parameter extraction according to (2.8).
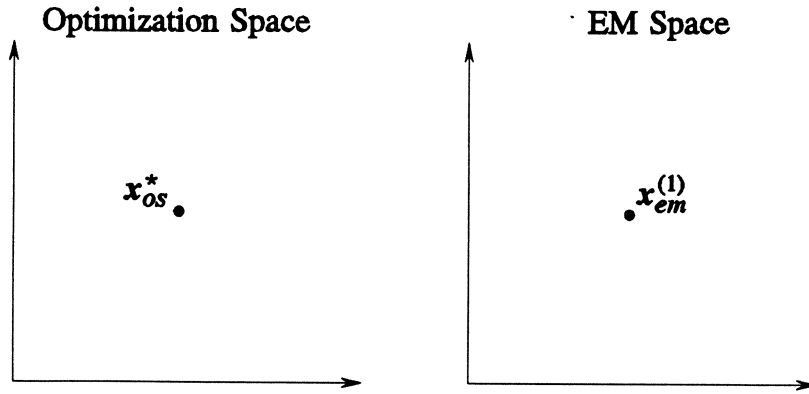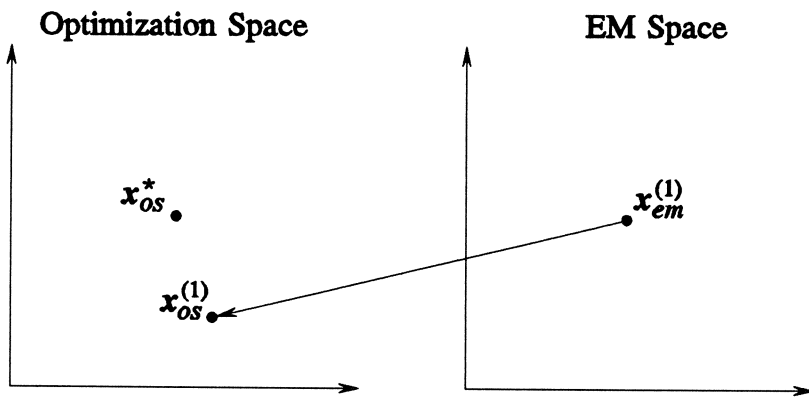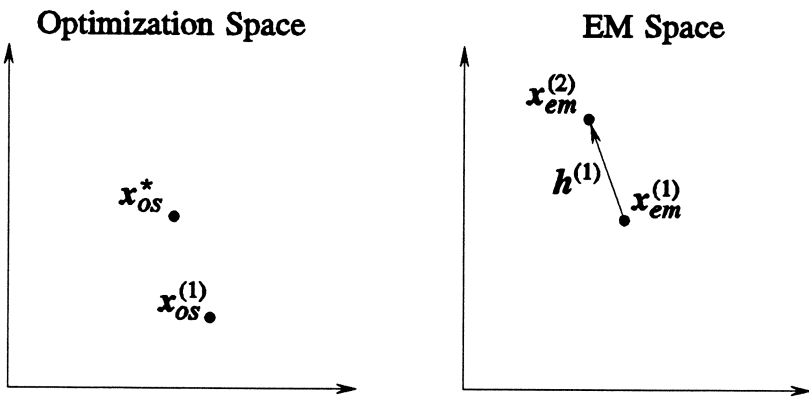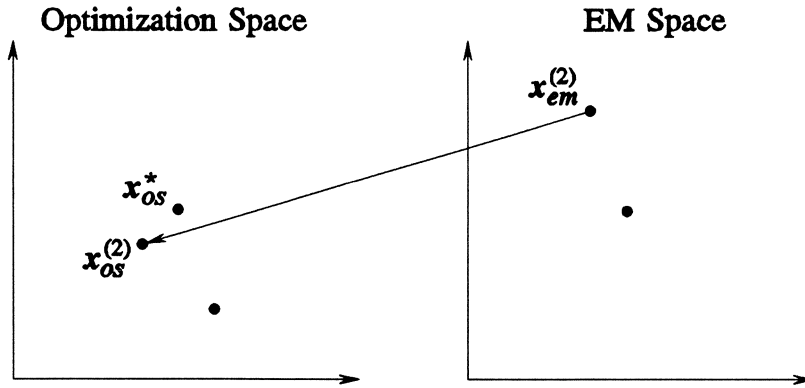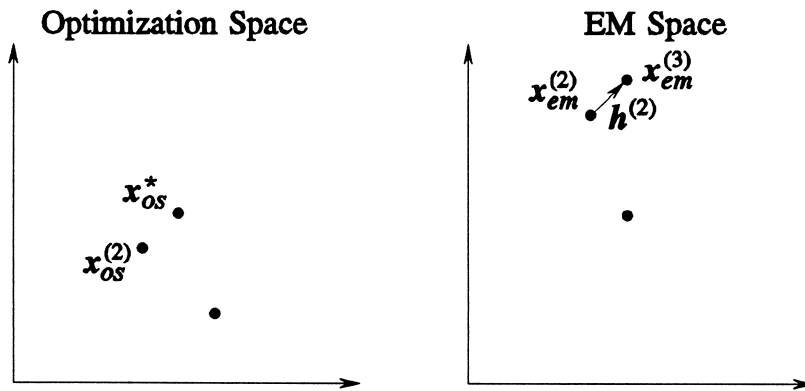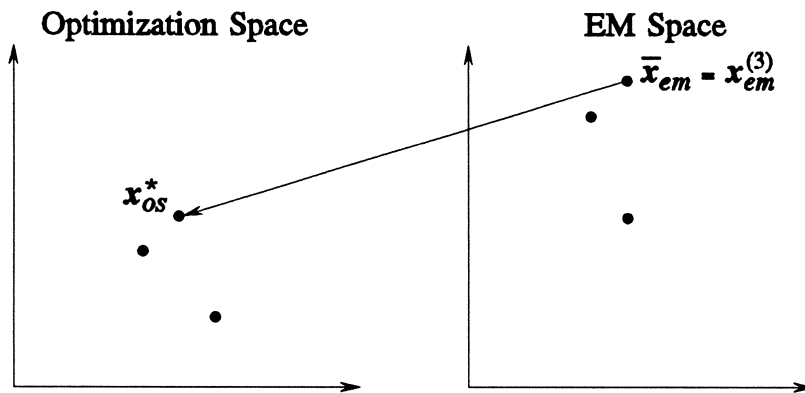
13
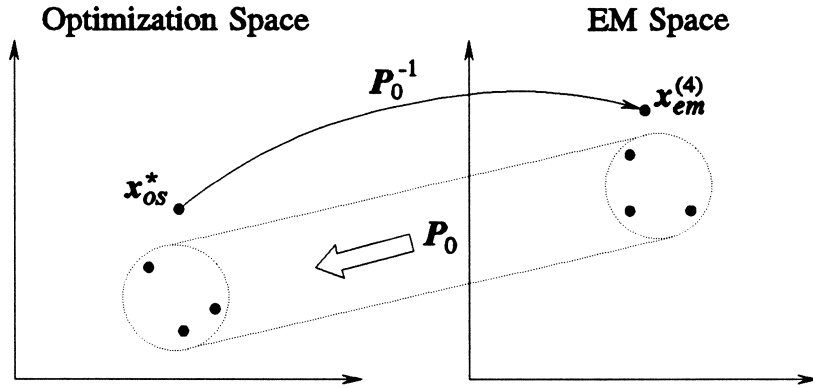
(d)
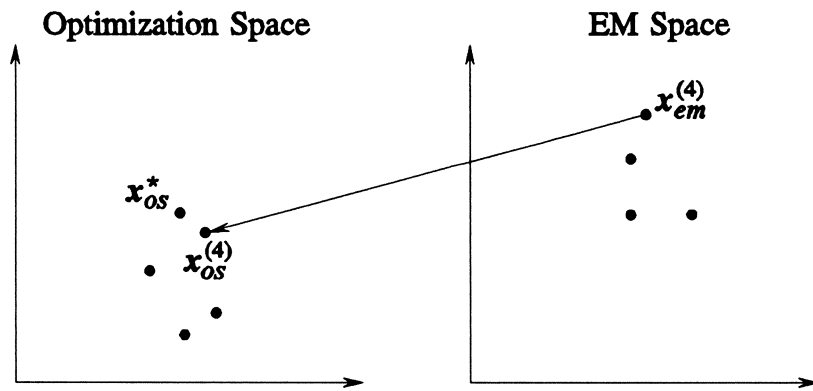
(e)
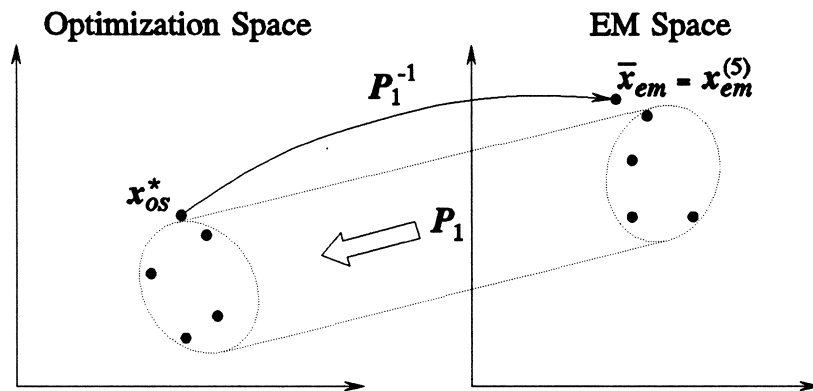
(f)

Fig. 1. Illustration of Space Mapping optimization (cont.): (d) use the inverse mapping to obtain $x_{em}^{(4)}$, (e) perform X_{os}-space model parameter extraction to obtain $x_{os}^{(4)}$, (f) apply the updated inverse mapping to obtain the SM solution $\bar{x}_{em} = x_{em}^{(5)}$, assuming $\| R_{os}(x_{os}^*) - R_{em}(x_{em}^{(5)}) \| \leq \epsilon$.

14

Optimization Space   **EM Space**

x_{os}^{*}

$x_{em}^{(1)}$

(a)

Optimization Space   **EM Space**

x_{os}^{*}

$x_{em}^{(1)}$

$x_{os}^{(1)}$

(b)

Optimization Space   **EM Space**

x_{os}^{*}

$x_{os}^{(1)}$

$x_{em}^{(2)}$

$h^{(1)}$

$x_{em}^{(1)}$

(c)

Fig. 2. Illustration of aggressive Space Mapping optimization: (a) set $x_{em}^{(1)} = x_{os}^{*}$ (assuming x_{em} and x_{os} represent the same physical parameters) and $B^{(1)} = 1$, (b) perform X_{os}-space model parameter extraction, (c) obtain $x_{em}^{(2)}$ by solving $B^{(1)}h^{(1)} = -f^{(1)}$.

15

Fig. 2.   Illustration of aggressive Space Mapping optimization (cont.):   (d) perform X_{os}-space model parameter extraction, (e) obtain $x_{em}^{(3)}$ by solving $B^{(2)}h^{(2)} = -f^{(2)}$, (f) the SM solution is $\overline{x}_{em} = x_{em}^{(3)}$ assuming $\| x_{os}^{(3)} - x_{os}^* \| \leq \eta$.
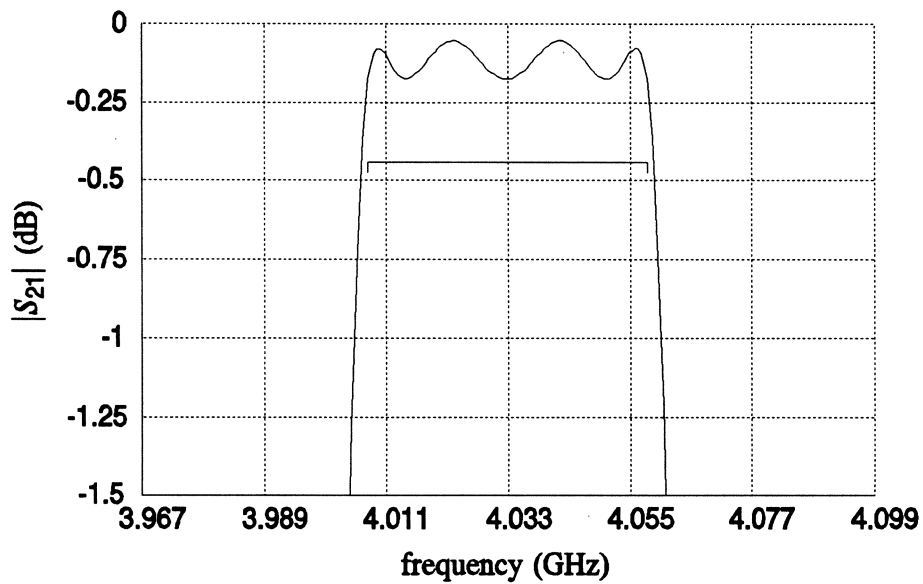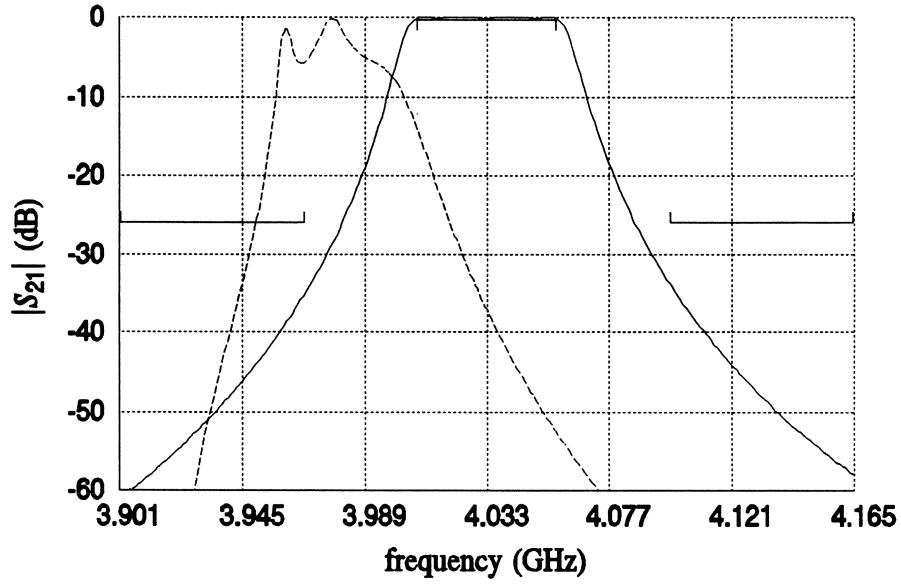
16
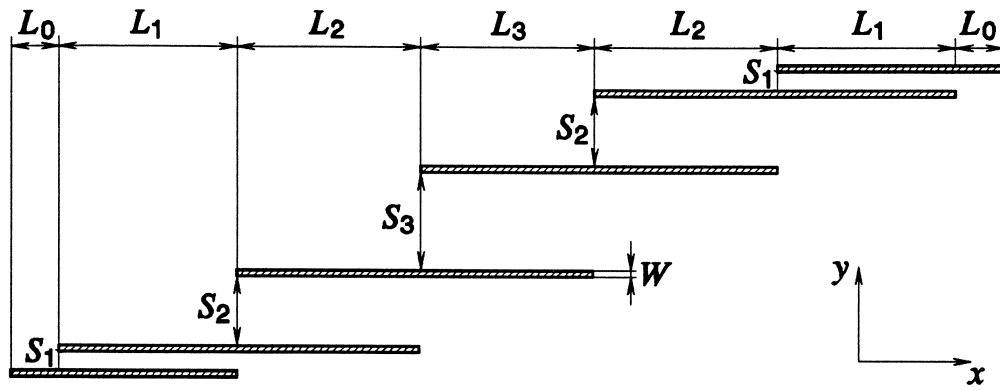
Fig. 3.   The structure of the HTS filter.
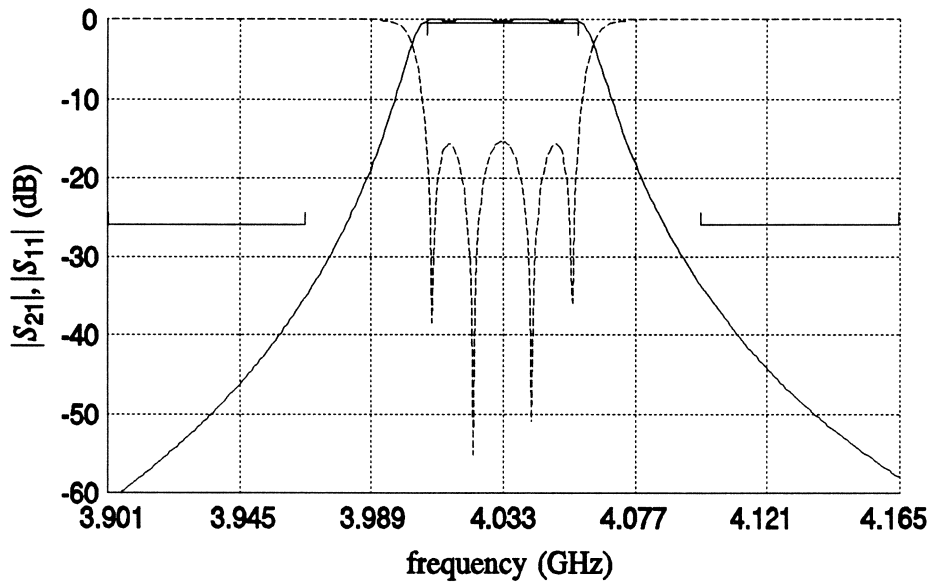
(a)

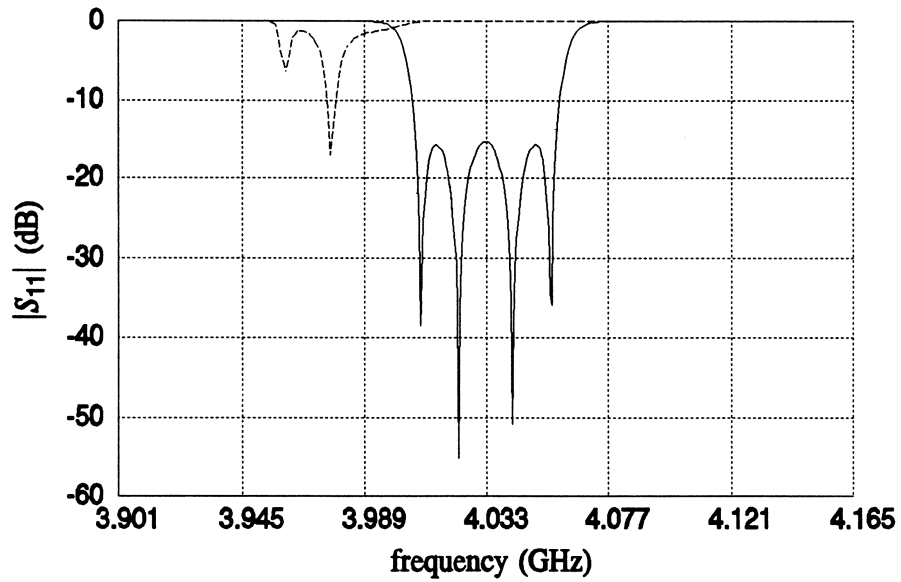

(b)

Fig. 4.   The OSA90/hope empirical model responses after minimax optimization. (a) $|S_{21}|$ (——) and $|S_{11}|$ (---) for the overall frequency band and (b) the passband details of $|S_{21}|$. ⌐⌐ and ⌐⌐ denote the upper and lower design specifications, respectively.
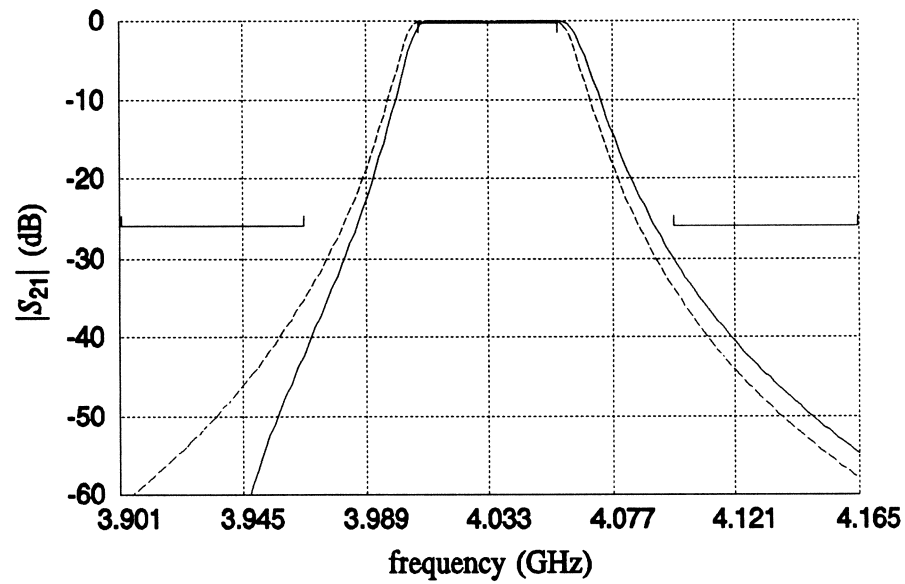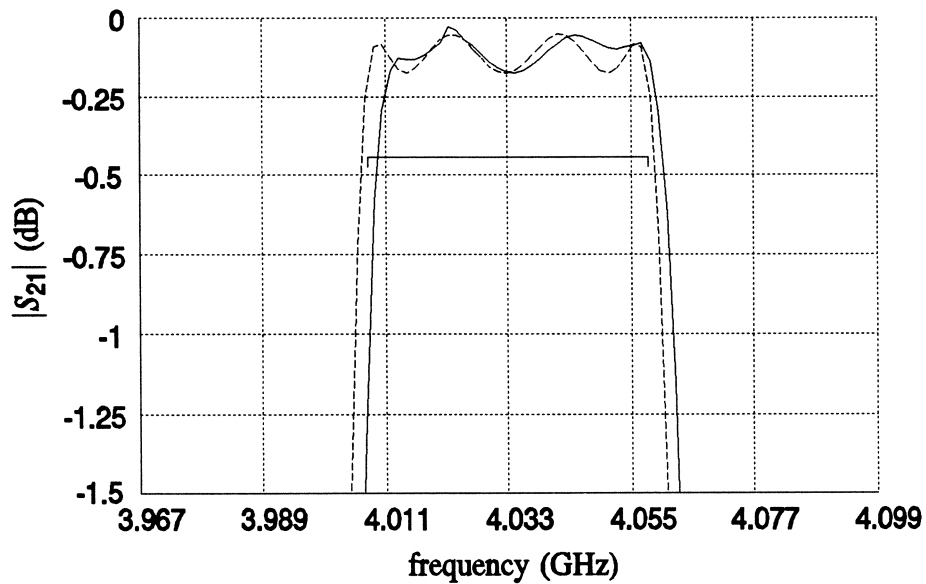
Fig. 5. A comparison of (a) $|S_{21}|$ and (b) $|S_{11}|$ between the empirical model (——) and *em* (---) at the empirical model minimax solution.
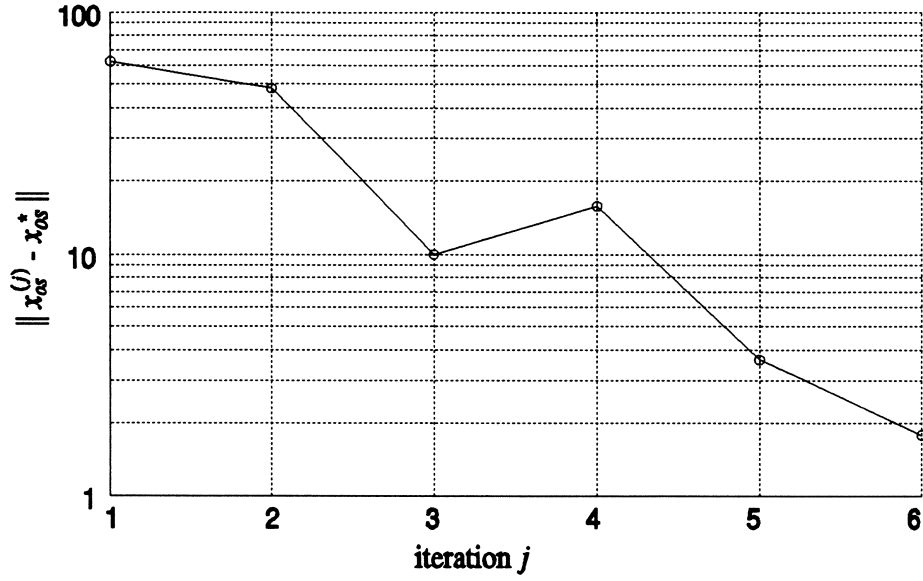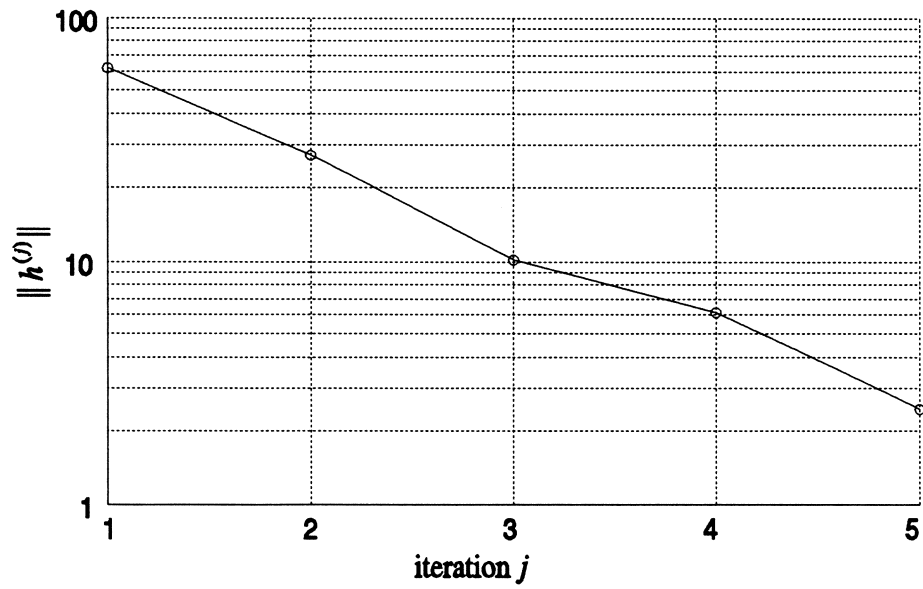
Fig. 6.   The *em* simulated $|S_{21}|$ response of the HTS filter at the SM solution obtained using the aggressive SM approach (——). The OSA90/hope empirical model solution (---) is shown for comparison. Responses are shown for (a) the overall frequency band and (b) the passband in more detail.

20

Fig. 7. Illustration of the progress of (a) $\| x_{os}^{(j+1)} - x_{os}^* \|_2$ and (b) $\| h^{(j)} \|_2$ corresponding to the aggressive SM optimization of the HTS filter.